The Journal of Neuroscience, March 1, 1996, 16(5):1702–1709

The Nitric Oxide/cGMP Pathway Couples Muscarinic Receptors to the Activation of Ca^{2+} Influx

Chris Mathes and Stuart H. Thompson

Department of Biological Sciences and the Hopkins Marine Station, Stanford University, Pacific Grove, California 93950

Inward currents activated by 8-bromo-cGMP and by muscarinic agonist were compared in N1E-115 mouse neuroblastoma cells using perforated-patch voltage clamp and Fura-2 imaging. The cGMP analog activates a voltage-independent inward current that is carried at least in part by Ca^{2+} because it persists in Na^{+}-free saline when Ca^{2+} is present and is blocked by external Mn^{2+} and Ba^{2+}. The current is similar to the inward current that develops during stimulation of M1 muscarinic receptors, and the currents activated by agonist and by 8-bromo-cGMP are not additive, indicating that the same pathway is involved. Inhibition of cGMP production with N_G-monomethyl-L-arginine (L-NMMA), a competitive inhibitor of nitric oxide (NO)-synthase, prevents activation of Ca^{2+} current by agonist without affecting the content of intracellular Ca^{2+} stores or the ability of agonist to mobilize Ca^{2+}. The inhibition is overcome by 8-bromo-cGMP. LY83583, a competitive inhibitor of guanylyl cyclase, reversibly blocks activation of Ca^{2+} current by agonist, again without affecting the content of Ca^{2+} stores or Ca^{2+} release. Rp-8-pCPT-cGMPS, an inhibitory analog of cGMP, also reduces the Ca^{2+} current and reduces Ca^{2+} influx during muscarinic activation. It is concluded that cGMP is the necessary and sufficient intermediate in the pathway linking muscarinic receptor occupancy to the activation of voltage-independent Ca^{2+} current. The pathway involves positive feedback. Calcium entering via voltage-independent channels preferentially stimulates NO-synthase, which leads to enhanced cGMP production and greater Ca^{2+} influx. Positive feedback may explain the rapid increase in cGMP that occurs during muscarinic receptor activation.

Key words: cGMP; nitric oxide; calcium current; muscarinic receptors; signal transduction; Ca^{2+} imaging

Muscarinic acetylcholine receptors stimulate multiple second-messenger pathways that can powerfully modify the physiological activity of neurons. We studied interactions between two of these pathways in N1E-115 mouse neuroblastoma cells. Stimulation of M1 receptors in this cell line causes rapid accumulation of cGMP. This requires Ca^{2+}/calmodulin-dependent activation of nitric oxide (NO)-synthase to produce the second-messenger NO, which in turn activates soluble guanylyl cyclase to produce cGMP (McKinney et al., 1990; Hu and El-Fakahany, 1993; Thompson et al., 1995). M1 receptors also activate phospholipase C-β via a G-protein, and this results in the production of inositol 1,4,5-trisphosphate (IP_3) and the subsequent release of Ca^{2+} into the cytosol from IP_3-sensitive intracellular Ca^{2+} stores. Intracellular Ca^{2+} release is one of two sources of Ca^{2+} required to stimulate cGMP production fully. The other source involves Ca^{2+} influx at the membrane by a pathway that is activated subsequent to Ca^{2+} release (Mathes and Thompson, 1994; Thompson et al., 1995). The Ca^{2+} influx pathway represents an important source of Ca^{2+} for refilling intracellular stores once the agonist action is terminated (Mathes and Thompson, 1995), but little is known about its regulation or modulation during muscarinic signal transduction. The work of Pandol and Schoeffield-Payne (1990), Bahnson et al. (1993), and Xu et al. (1994) suggested that cGMP may be responsible for linking Ca^{2+} release from internal stores to the activation of voltage-independent Ca^{2+} current in pancreatic acinar cells. Because muscarinic activation of N1E-115 cells dramatically elevates the intracellular cGMP concentration, we considered the possibility that cGMP might activate Ca^{2+} current in this excitable cell line as well. This was explored using nystatin perforated-patch voltage clamp and Fura-2 imaging.

We found that 8-bromo-cGMP, a membrane permeable analog of cGMP, activates a voltage-independent Ca^{2+} current with properties similar to the current activated by muscarinic agonists. Inhibitors of cGMP formation or the binding of cGMP to its effectors prevents activation of the current by agonist without affecting intracellular Ca^{2+} release or the content of calcium stores. We conclude that cGMP is the factor necessary for coupling muscarinic receptor occupancy to the activation of Ca^{2+} current. It is apparent that the IP_3-signaling pathway and the cGMP pathway interact at the level of intracellular Ca^{2+} concentration. This interaction represents a positive-feedback loop linking increases in intracellular calcium ($[Ca]_i$) to increased production of cGMP and increased Ca^{2+} influx. Positive feedback helps to explain the rapid increase in cGMP production (and by inference, NO production) that occurs during muscarinic receptor activation.

MATERIALS AND METHODS

Cell culture. The N1E-115 neuroblastoma cell line, derived from mouse sympathetic ganglion neurons (Amano et al., 1972), was obtained from the University of California San Francisco Cell Culture Facility and used in passages 3–8. Cells were grown in DMEM with 10% fetal bovine serum (HyClone, Logan, UT) at 37°C in a 10% CO_2 atmosphere, plated on glass coverslips, and grown to ~80% confluence before differentiation with dimethyl sulfoxide (DMSO) for 5–21 d (Kimhi et al., 1976). Plated cells were fed every 2–3 d and used 1–2 d after feeding.

Received Sept. 18, 1995; revised Dec. 8, 1995; accepted Dec. 15, 1995.

This work was supported by National Institutes of Health Grant NS14519 (S.H.T.), a predoctoral fellowship from the American Foundation for Aging Research (C.M.), and National Institutes of Health Grant MH10425 (C.M.). We thank C. E. Thompson for her timely arrival, Drs. A. A. Alousi, J. S. Coggan, I. Kovacs, and S. S.-H. Wang for critical comment and discussion, and we thank R. Kramer and G. R. Tibbs for sharing their unpublished data.

Correspondence should be addressed to Stuart Thompson at the above address.

Solutions and chemicals. Experiments were carried out at a temperature of 30°C. The external saline solution contained (in mM): 146 NaCl, 5.4 KCl, 1.8 $CaCl_2$, 0.8 $MgSO_4$, 0.4 KH_2PO_4, 0.3 Na_2HPO_4, 5 glucose, and 20 HEPES, plus 10 μM curare and 1 μM tetrodotoxin (TTX), pH 7.4. The Na^+-free, high-Ca^{2+} saline contained (in mM): 90 Tris-HCl, 5.4 KCl, 25 $CaCl_2$, 0.8 $MgSO_4$, 10 tetraethylammonium (TEA) chloride, 5 glucose, and 25 HEPES, plus 10 μM D-tubocurarine and 1 μM TTX. The bath volume (500 μl) was exchanged with a gravity perfusion system (half-time for exchange ~2 sec). Carbachol was dissolved in saline and applied at a final concentration of 1 mM (EC_{50} for Ca^{2+} release = 100 μM) (Wang and Thompson, 1994). N^G-monomethyl-L-arginine (L-NMMA), N^G-monomethyl-D-arginine (D-NMMA), and 6-anilinoquinoline-5,8-quinone (LY83583) were from Calbiochem (La Jolla, CA). Rp-8-pCPT-cGMPS was from BioLog (La Jolla, CA). All other chemicals were from Sigma (St. Louis, MO). LY83583 was dissolved in DMSO and diluted to the appropriate concentration on the day of the experiment.

Nystatin-patch clamp. The nystatin perforated-patch technique was used for whole-cell voltage clamp (Horn and Marty, 1988). The pipette solution contained (in mM): 16 CsCl, 70 Cs_2SO_4, 5 $MgSO_4$, 10 HEPES, 0.05% Pluronic F-127 (Molecular Probes, Eugene, OR), and 100 sucrose (~320 mOsM), pH 7.2. With this pipette solution, the calculated equilibrium potential for Cl^- for cells bathed in normal saline was −60 mV, assuming finite permeability of nystatin to Cl^- and adequate time for equilibration. Nystatin was added to filtered pipette solution from a DMSO stock (2.5 mg nystatin in 50 μl DMSO) to a final concentration of 100–200 μg/ml, and this solution was used within the hour. Patch electrodes were made from Borofilament glass (Sutter Instrument, Novato, CA). Membrane currents were recorded using a List EPC-7 amplifier and PClamp software. Series resistance ranged from 20 to 40 mΩ, and ~50% compensation was used, allowing the cell capacitance to be compensated adequately. A holding voltage of −60 mV was used, which is near the normal resting potential.

Ca^{2+} imaging. Cells were loaded with the Ca^{2+} indicator Fura-2 by incubation in saline containing 5 μM Fura-2/AM and 0.025% Pluronic F-127 for 1 hr at 22°C. After the cells were rinsed, they were transferred to a heated chamber (30°C) on the stage of a Nikon Diaphot equipped with a 20× Fluor objective, Hamamatsu C2400 SIT camera and a Sony videotape recorder. Xenon arc illumination was filtered through 10 nm bandpass interference filters with 340 and 380 nm center wavelengths. Calibration of fluorescence to units of Ca^{2+} was performed off-line using a pipeline image processor (Megavision, Santa Barbara, CA). Background-subtracted and frame-averaged F_{340}/F_{380} ratios were calibrated using standard solutions between two coverslips, according to the equations of Grynkiewicz et al. (1985). Intracellular Ca^{2+} concentrations were measured in regions of interest corresponding to the interiors of individual cell bodies. Calcium kinetics were resolved by monitoring cells continuously for up to 2 min with 380 nm excitation after first obtaining F_{340}/F_{380}. Because dye fade during this period was insignificant, only an initial ratiometric determination was needed at the beginning of each record. The initial F_{380} and $[Ca]_i$ in individual cells allowed the calculation of F_{min} and F_{max}, corresponding to zero and saturating Ca^{2+} concentrations, using the equations:

$$F_{max} = F_{380}\,(1 + (Ca)_i/K_D)/(\sigma + (Ca)_i/K_D)$$

$$F_{min} = \sigma \times F_{max},$$

where $\sigma = F_{380,min}/F_{380,max}$ and σ is a constant of the imaging system. $[Ca]_i$ at later times could then be calculated from F_{380} using the Henderson–Hasselbalch equation, as is done for single-wavelength dyes (Kao et al., 1989). The values of the calibration parameters R_{min}, R_{max}, and σ were 0.056, 4.85, and 22.66, respectively.

RESULTS

Inward current activated by 8-bromo-cGMP

Application of 8-bromo-cGMP, a membrane-permeable analog of cGMP, activates inward membrane current in N1E-115 mouse neuroblastoma cells. An example measured with permeabilized-patch voltage clamp is shown in Figure 1*A*. When 1 mM 8-bromo-cGMP was introduced in normal external saline with 1 μM TTX, an inward current gradually developed that reached a current density of 0.41 pA/pF after 15 min at the −60 mV holding potential. The slow onset of the current probably results from gradual entry of the cyclic nucleotide into the cell and is consistent with an intracellular site of action. The cyclic nucleotide also activates inward current in cells bathed in Na^+-free, high-Ca^{2+} saline containing 25 mM Ca^{2+}, indicating that substantial current can be carried by Ca^{2+} (Fig. 1*B*) (current density = 0.63 pA/pF after 15 min). The inward current is reversibly blocked by 2 mM external Mn^{2+} or 2 mM Ba^{2+}, whether the cells are bathed in normal saline or in Na^+-free, high-Ca^{2+} saline (Fig. 1*B*).

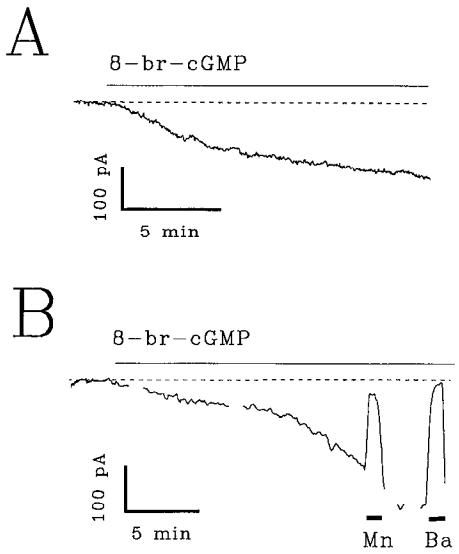

Figure 1. 8-bromo-cGMP activates a voltage-independent inward current. *A*, Membrane current measured with nystatin-patch clamp during addition of 1 mM 8-bromo-cGMP dissolved in normal saline (holding voltage = −60 mV; a *dashed line* is drawn through the initial holding current; cell capacitance, 360 pF; R_s = 38 MΩ). The agonist was applied at the time indicated by the *solid bar*. *B*, Inward current activated by 8-bromo-cGMP (1 mM) in a cell bathed in Na^+-free, high-Ca^{2+} saline and voltage-clamped to −60 mV. At the time indicated by the *bar*, the chamber was rinsed with Na^+-free saline plus 1 mM 8-bromo-cGMP. After 17 min, the chamber was rinsed again with the same saline plus 2 mM Mn^{2+} (*Mn*) for a period of 1 min before returning to the original Na^+-free saline. The procedure was repeated 3 min later using 2 mM Ba^{2+} (*Ba*) in place of Mn^{2+}. Interruptions in the record correspond to times when voltage-clamp pulses were applied to measure the *I–V* curve.

The difference current–voltage (*I–V*) curve for the cyclic nucleotide-dependent current in high-Ca^{2+} saline is shown in Figure 2. The points were obtained by subtracting control currents measured during pulses to voltages between −95 and −50 mV from currents measured during the same pulse series 15 min after adding 1 mM 8-bromo-cGMP. Difference currents calculated in this way changed instantaneously during voltage steps without evidence of time-dependent gating, indicating that the activation process is not voltage dependent within this range. The positive slope of the *I–V* curve shows that the cyclic nucleotide causes a conductance increase, but it was not possible to extend the curve to voltages more positive than −50 mV or to measure a reversal potential, because other strongly voltage-dependent Ca^{2+} currents begin to activate with larger steps (Yoshii et al., 1988). Because the cGMP-dependent current is expected to be a minor component of the total Ca^{2+} current at depolarized voltages, it was not practical to use a pharmacological approach to isolate it. The dashed line in Figure 2 is the expected *I–V* curve for a Ca^{2+} current calculated from the Goldman–Hodgkin–Katz current equation, with extracellular calcium ($[Ca]_o$) equal to 25 mM and

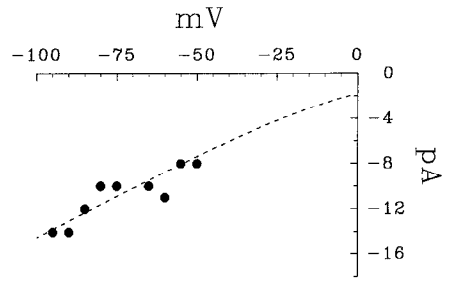

Figure 2. Difference *I–V* curve in high-Ca^{2+} saline. A series of 300 msec pulses to voltages between −95 and −50 mV was applied from a holding voltage of −60 mV before and 15 min after applying 1 mM 8-bromo-cGMP. The experiment was carried out in Na^+-free, high-Ca^{2+} saline containing 10 mM TEA and 1 μM TTX. Data points were obtained by subtracting the steady-state current measured during each step in normal saline from the current during the corresponding step in cGMP. The *dashed line* shows the expected *I–V* curve for a Ca^{2+} current calculated from the Goldman–Hodgkin–Katz current equation assuming $[Ca]_i$ = 70 nM and $[Ca]_o$ = 25 mM.

$[Ca]_i$ equal to 70 nM. This provides a reasonable approximation to the data and suggests a reversal potential more positive than +40 mV. Because the *I–V* curve was measured in Na^+-free external saline, Na^+ is excluded as the carrier of inward current. Contamination from potassium currents is minimal because the pipette solution contained 156 mM Cs^+ in place of K^+, and the external saline contained 10 mM TEA to suppress currents flowing in potassium channels. In addition, the calculated equilibrium potential for Cl^- is −60 mV, equivalent to the holding potential. Under these conditions, Ca^{2+} is the most likely candidate to carry the cyclic nucleotide-dependent inward current. For these reasons, and because the current is blocked by Mn^{2+} and Ba^{2+}, we conclude that Ca^{2+} carries a significant fraction of the current activated by 8-bromo-cGMP, even in normal saline.

The amplitudes of cyclic nucleotide-dependent inward currents measured in normal saline (average current density = 0.40 ± 0.12 pA/pF, mean ± SEM; n = 8) and high-Ca^{2+} saline (0.27 ± 0.18 pA/pF; n = 3) were not statistically different (p = 0.6, two-tailed t test). This does not match the simple expectation for a Ca^{2+}-selective current because one would expect the current density at a particular voltage to increase as the external Ca^{2+} concentration is raised. One possible explanation is that the current may saturate at Ca^{2+} concentrations above the physiological level in a manner similar to what is seen with voltage-dependent Ca^{2+} channels (Almers and McCleskey, 1984; Hess and Tsien, 1984). Alternatively, the pathway may be permeable to both Na^+ and Ca^{2+} with a conductance that depends on the ratio of permeant ion concentrations (Hagiwara, 1983; Hess and Tsien, 1984). The present data are not sufficient to decide between these alternatives.

8-Bromo-cGMP increases Ca^{2+} influx

Fura-2 fluorescence imaging was used to measure changes in intracellular Ca^{2+} concentration during the application of 8-bromo-cGMP. Figure 3*A* shows an example from a single cell bathed in normal saline; the result is representative of 20 experiments. Calcium concentration was measured ratiometrically at successive time points before and after adding 1 mM 8-bromo-cGMP to the bath. The figure shows that $[Ca]_i$ increased from a resting value of ~40 nM to ~120 nM within 15 min. The time course of this increase is approximately the same as the time course of inward current activation measured with nystatin-patch

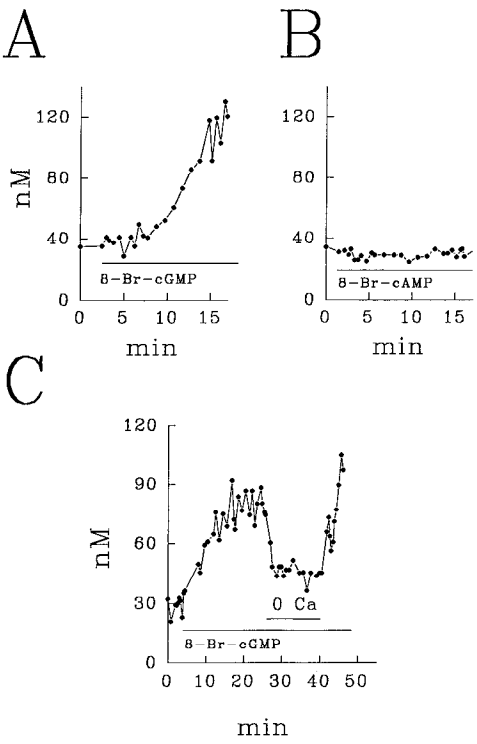

Figure 3. Fura-2 imaging shows that 8-bromo-cGMP elevates $[Ca]_i$. *A*, Measurement of $[Ca]_i$ in a single cell loaded with Fura-2/AM and bathed in normal saline containing 1.8 mM Ca^{2+}. At the time marked by the *bar*, 1 mM 8-bromo-cGMP was added to the bath. Each point represents a ratiometric determination of $[Ca]_i$. *B*, The same experiment was repeated with 1 mM 8-bromo-cAMP, and the result shows that cAMP does not elevate $[Ca]_i$ (representative of 10 experiments). *C*, The elevation in $[Ca]_i$ during exposure to 8-bromo-cGMP is attributable to Ca^{2+} influx. Ratiometric imaging applied to a cell bathed in normal saline; 1 mM 8-bromo-cGMP was applied at the time marked by the *bar*. Twenty-five minutes later, the chamber volume was replaced with saline containing 70 nM free Ca^{2+} plus 1 mM 8-bromo-cGMP for 15 min. At the end of this time, normal saline containing 1.8 mM Ca^{2+} plus 1 mM 8-bromo-cGMP was returned.

voltage clamp, which supports the conclusion that the inward current activated by 8-bromo-cGMP is carried in part by Ca^{2+}. This effect was specific for cGMP because bath application of 1 mM 8-bromo-cAMP under the same conditions did not change $[Ca]_i$ in any of the 10 experiments (Fig. 3*B*).

The increase in intracellular Ca^{2+} concentration results from increased Ca^{2+} influx. In the example in Figure 3*C*, the cell was exposed first to normal saline containing 1 mM 8-bromo-cGMP. After 20 min, the external saline was exchanged for one containing the same concentration of cyclic nucleotide but a much lower Ca^{2+} concentration (1.8 mM Ca^{2+} plus 4 mM EGTA; 70 nM free Ca^{2+}), which resulted in a decrease in $[Ca]_i$ toward the resting level. This was reversed when normal saline was reintroduced. This result is representative of experiments on 20 cells and shows that the $[Ca]_i$ increase caused by 8-bromo-cGMP is the result of Ca^{2+} influx from the extracellular compartment rather than Ca^{2+} release from intracellular stores.

The NO generator sodium nitroprusside (SNP) stimulates cGMP production in N1E-115 cells (McKinney et al., 1990; Thompson et al., 1995). We found that 100 μM SNP, dissolved in normal saline, also causes the intracellular Ca^{2+} concentration to increase rapidly, reaching a value of 47 ± 16 nM (mean ± SEM;

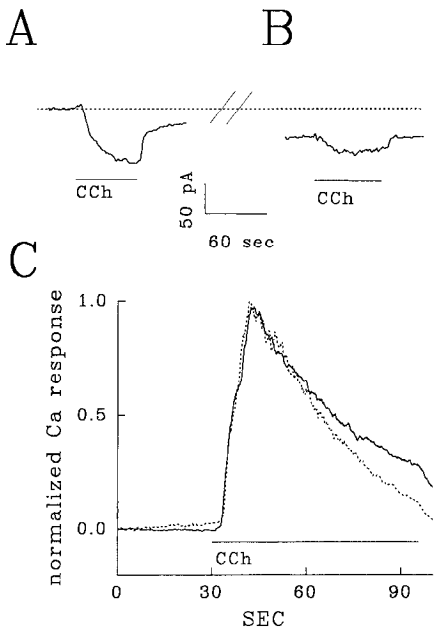

Figure 4. The inward currents activated by carbachol and 8-bromo-cGMP are not additive. *A*, Membrane current measured with nystatin-patch clamp (holding voltage = −60 mV; normal saline). The initial holding current is shown by the *dashed line*; 1 mM carbachol (*CCh*) was applied for 1 min at the time indicated by the *bar*. The inward current amplitude was 83 pA. *B*, The agonist was rinsed away, and 1 mM 8-bromo-cGMP was added to the external saline. The cyclic nucleotide activated an inward current of 56 pA. After 15 min, carbachol (*CCh*) was applied a second time and caused an increment in inward current of 21 pA. *C*, Fura-2 imaging shows that incubation with 8-bromo-cGMP reduces the late phase of the Ca^{2+} response to carbachol (*CCh*). Cells loaded with Fura-2/AM were stimulated twice with 1 mM carbachol (exposure to carbachol indicated by the *bar*). During the first stimulation, the cells were bathed in normal external saline. The *solid line* shows the average Ca^{2+} response (n = 10). After rinsing, the saline was exchanged for one containing 1 mM 8-bromo-cGMP. After 15 min, 1 mM carbachol was applied a second time. The Ca^{2+} response (*dashed line*) was corrected for the change in basal $[Ca]_i$ level and normalized to the peak of the control response.

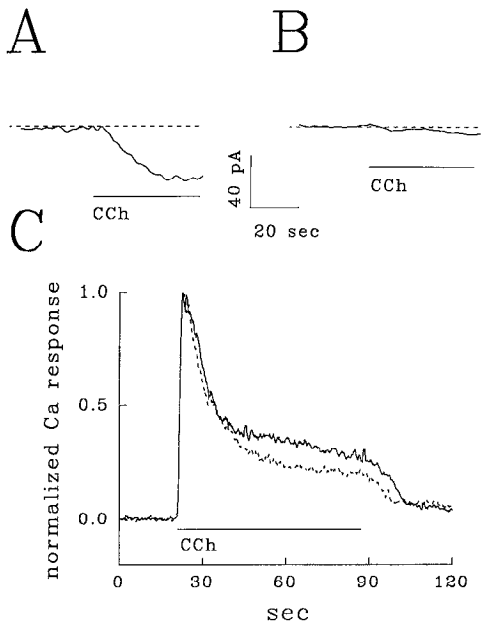

Figure 5. L-NMMA, a competitive inhibitor of NO-synthase, prevents activation of inward current by carbachol. *A*, Membrane current in a cell bathed in normal external saline during stimulation with 1 mM carbachol (*CCh*; agonist application indicated by the *bar*; holding voltage = −60 mV). *B*, The agonist was rinsed from the bath and replaced with saline containing 100 μM L-NMMA. After 15 min, 1 mM carbachol dissolved in saline plus 100 μM L-NMMA was applied a second time. *C*, Fura-2 imaging shows that L-NMMA reduces the plateau in the Ca^{2+} response to carbachol. Cells loaded with Fura-2 and bathed in normal saline were stimulated with 1 mM carbachol for the period indicated. The average response is shown by the *solid line* (n = 10). The agonist was rinsed from the chamber with saline containing 100 μM L-NMMA. After 15 min, the cells were stimulated a second time with 1 mM carbachol (dissolved in saline plus L-NMMA), and the responses were averaged (*dashed line*). The responses were normalized to the same peak amplitude.

n = 9) above the resting level within 90 sec. Incubation with 100 μM SNP for periods as long as 5 min had no effect on the peak amplitude of the Ca^{2+} response to carbachol. Because the peak $[Ca]_i$ change reflects intracellular Ca^{2+} release rather than Ca^{2+} influx (Mathes and Thompson, 1994), this finding shows that SNP does not alter the Ca^{2+} content of the IP_3-releasable Ca^{2+} pool or the ability of agonist to stimulate Ca^{2+} release. These experiments provide further evidence that stimulation of the NO/guanylyl cyclase pathway is sufficient to activate Ca^{2+} influx.

cGMP and muscarinic agonist activate the same inward current

The inward current activated by 8-bromo-cGMP has several properties in common with the voltage-independent inward current activated by muscarinic agonist. In both cases the current is carried in part by Ca^{2+}, and the currents reach approximately the same maximum current density. Both currents are susceptible to block by external Mn^{2+} and Ba^{2+}, a property that is distinctly different from the other highly voltage-dependent Ca^{2+} channels expressed in these cells (Mathes and Thompson, 1994). These observations suggest that cGMP and muscarinic agonists might activate the same pathway. If this were so, we would expect that cGMP would compete with carbachol for activation of the current and thereby reduce the increment in current amplitude that occurs when carbachol is applied. Figure 4 shows the results of a voltage-clamp experiment designed to test this prediction. In *A*, the current in response to 1 mM carbachol reached a steady amplitude of 83 pA. The agonist was washed away, and the cell was incubated in saline containing 1 mM 8-bromo-cGMP. This resulted in an inward current that reached 56 pA after 15 min. Carbachol was applied a second time in the presence of 8-bromo-cGMP, and now the agonist activated an inward current of 21 pA, 25% of the control current amplitude. The decrease in the carbachol response is in approximate proportion to the inward current activated by 8-bromo-cGMP. In three experiments, the average decrease in the carbachol response after 15 min in 1 mM 8-bromo-cGMP was 91 ± 11% (mean ± SD).

The observation that the inward currents activated by 8-bromo-cGMP and by carbachol do not sum is consistent with the hypothesis that cGMP and agonist activate the same pathway. This was tested further in a Fura-2 imaging experiment. The Ca^{2+} response to 1 mM carbachol was recorded in the same group of 10 cells, first under control conditions and then after a 15 min incubation with 1 mM 8-bromo-cGMP. The cyclic nucleotide caused a 50–100 nM increase in $[Ca]_i$ in different cells. The average peak amplitude of the response to the second carbachol application was 8% smaller than the first response, which is approximately the decrease ex-

Table 1. Effects of inhibitors of cGMP production on inward current

	pA	pA/pF
Control	99 ± 16 (n = 3)	0.34 ± 0.04
L-NMMA	4 ± 4 (n = 4)	0.02 ± 0.02*
Control	86 ± 34 (n = 5)	0.28 ± 0.14
D-NMMA	88 ± 35 (NS) (n = 6)	0.28 ± 0.16 (NS)
Control	42 ± 29 (n = 3)	0.13 ± 0.05
LY 83583	0 ± 0 (n = 3)	0 ± 0*
Control	49 ± 30 (n = 5)	0.21 ± 0.10
10 μM Rp-8-pCPT-cGMPs	14 ± 9 (n = 4)	0.06 ± 0.04*

*$p < 0.01$ (matched pairs t-test applied to percentage change in current density). NS, not significant at the 0.05 level.

pected from muscarinic receptor desensitization under control conditions (Wang and Thompson, 1994; Mathes and Thompson, 1995). We showed previously that the peak increase in $[Ca]_i$ is attributable to Ca^{2+} release from internal stores and that Ca^{2+} influx does not contribute to the signal until after the peak (Mathes and Thompson, 1994). The observation that the peak $[Ca]_i$ increase does not change more than expected from desensitization makes two points. It shows that 8-bromo-cGMP does not inactivate the agonist receptor or the intermediate steps in the signaling cascade that lead to intracellular Ca^{2+} release. It also shows that the cyclic nucleotide does not by itself deplete intracellular stores of Ca^{2+}. This is important because store depletion could cause the production of an independent factor, unrelated to cGMP, that could act as a second messenger to activate a refilling Ca^{2+} current (Putney and Bird, 1993). Figure 4*C* shows the average calcium signal during the application of carbachol under control conditions (*solid line*) and after 8-bromo-cGMP (*dashed line*). The change in basal $[Ca]_i$ was subtracted and the responses were normalized to the same peak amplitude to emphasize the change in waveform. The Ca^{2+} signal decays more rapidly in cells treated with cGMP than in control cells. Calcium influx normally contributes to the Ca^{2+} signal at this late stage, prolonging the falling phase of the response (Mathes and Thompson, 1994). Because the response waveform does not change during repeated applications of agonist under control conditions, the increased rate of decay of $[Ca]_i$ is a result of the exposure to cyclic nucleotide (Wang and Thompson, 1994). Our interpretation is that incubation with 8-bromo-cGMP activates Ca^{2+} influx toward saturation and thereby reduces the further activation of Ca^{2+} influx by agonist. The decrease in the late phase of the $[Ca]_i$ response to agonist by previous exposure to 8-bromo-cGMP supports the hypothesis that cGMP and carbachol activate the same Ca^{2+} influx pathway.

The activation of Ca^{2+} influx by muscarinic agonist is prevented by inhibitors of NO-synthase

In this cell line, activation of M1 receptors by carbachol causes a rapid increase in cGMP. cGMP production is prevented when

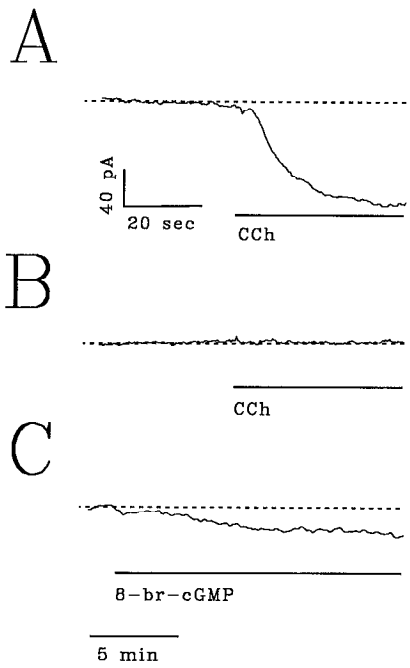

Figure 6. L-NMMA does not prevent the activation of inward current by 8-bromo-cGMP. *A*, Nystatin-patch recording of membrane current activated by 1 mM carbachol (*CCh*) (agonist application indicated by *bar*; normal saline; −60 mV holding potential). *B*, The agonist was washed from the chamber, and saline containing 100 μM L-NMMA was added. After 15 min, 1 mM carbachol (*CCh*) was applied a second time and failed to elicit a response. *C*, The agonist was rinsed from the chamber, again with saline containing 100 μM L-NMMA, and 15 min later saline containing 1 mM 8-bromo-cGMP plus 100 μM L-NMMA was added. The records were extracted from a continuous recording from the same neuron.

NO-synthase is blocked with the competitive inhibitor L-NMMA (McKinney et al., 1990; Thompson et al., 1995), and in the present experiments we found that L-NMMA also prevents the activation of Ca^{2+} influx by carbachol. An example is shown in Figure 5. Application of 1 mM carbachol under control conditions activated an inward current that reached an amplitude of 43 pA (Fig. 5*A*). The cell was incubated in saline containing 100 μM L-NMMA for 15 min before carbachol was applied a second time. On the second application, the agonist elicited an inward current of 5 pA, equal to 11% of the control value (Fig. 5*B*). In four experiments with 100 μM L-NMMA, the inhibitor reduced the inward current by 96 ± 9% (mean ± SD) (Table 1). Identical treatment with the inactive isomer D-NMMA had no effect on the activation of inward current by carbachol (Table 1). 8-Bromo-cGMP is able to activate inward current in the presence of L-NMMA. In the example illustrated in Figure 6, carbachol activated an inward current of 106 pA under control conditions (*A*). After a 15 min incubation with 100 μM L-NMMA, a second application of carbachol failed to activate inward current, indicating that the pathway was completely blocked (*B*). The agonist was rinsed from the chamber, and 1 mM 8-bromo-cGMP was added in the continued presence of L-NMMA. This resulted in a gradual increase in inward current that reached 35 pA after 15 min (*C*), indicating that the cyclic nucleotide can bypass the NO pathway to activate the current directly.

Fura-2 imaging experiments showed that inhibition of NO-synthase with L-NMMA reduces Ca^{2+} influx in response to muscarinic agonist. Figure 5*C* shows the average change in $[Ca]_i$ in 10

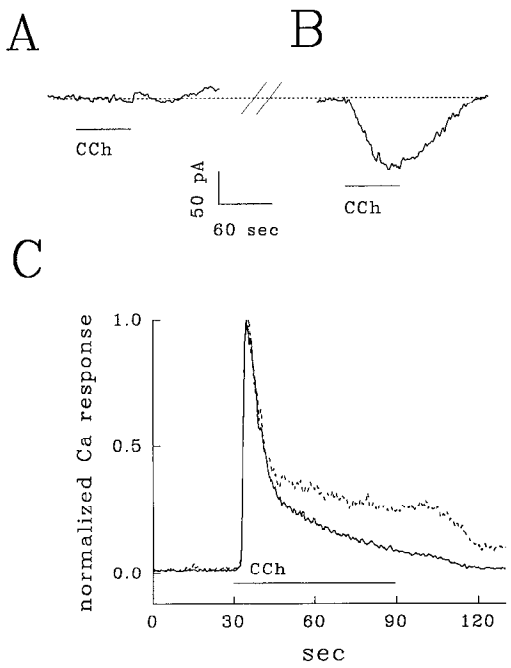

Figure 7. The reversible guanylyl cyclase inhibitor LY83583 blocks activation of inward current by carbachol. *A*, Membrane current in a cell incubated with 10 μM LY83583 for 15 min and voltage-clamped to −60 mV; 1 mM carbachol (*CCh*) dissolved in saline plus 10 μM LY83583 was applied at the time indicated by the *bar*. *B*, The agonist and LY83583 were washed from the chamber with normal saline, and after 15 min 1 mM carbachol (*CCh*) was applied a second time. *C*, Fura-2 imaging shows that LY83583 reduces the plateau in the Ca^{2+} response to carbachol (*CCh*). Cells loaded with Fura-2 were incubated with saline containing 10 μM LY83583 for 15 min before stimulating with 1 mM carbachol dissolved in the same saline. The average Ca^{2+} response is shown by the *solid line* ($n = 10$; carbachol stimulation indicated by the *bar*). The inhibitor was rinsed from the chamber with normal saline. After 15 min, 1 mM carbachol was applied a second time, and the average response in the same 10 cells is shown by the *dashed line* (normalized by peak amplitude).

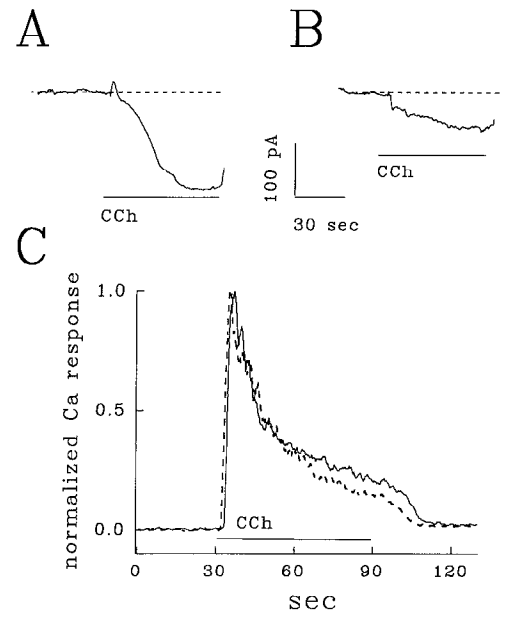

Figure 8. Rp-8-pCPT-cGMPS, an inhibitory analog of cGMP, reduces the activation of inward current by carbachol. *A*, Membrane current recorded with nystatin-patch clamp during the application of 1 mM carbachol (*CCh*; time shown by the *bar*) to a cell bathed in normal saline (holding voltage = −60 mV). *B*, Membrane current during a second agonist application after 15 min incubation in saline containing 10 μM Rp-8-pCPT-cGMPS. *C*, Fura-2 imaging shows that Rp-8-pCPT-cGMPS reduces the plateau in the Ca^{2+} response to agonist. The response to 1 mM carbachol (*CCh*) in a single cell bathed in normal saline is shown by the *solid line*. The agonist was rinsed away, and saline with 100 μM Rp-8-pCPT-cGMPS was added. After 15 min, the agonist was applied a second time in the presence of inhibitor (*dashed line*; normalized by peak amplitude).

cells during carbachol stimulation under control conditions (*solid line*). The falling phase of the Ca^{2+} signal is characterized by a plateau that results from Ca^{2+} influx (Mathes and Thompson, 1994). After the agonist was washed away, the cells were incubated with 100 μM L-NMMA for 15 min before carbachol was applied a second time (*dashed line*; normalized to the peak of the control response). This had no effect on the basal level of $[Ca]_i$. The peak amplitude of the Ca^{2+} response during the second agonist application was reduced by 11%, a decrease within the range expected from muscarinic receptor desensitization. L-NMMA caused a greater decrease in the plateau, which is consistent with inhibition of Ca^{2+} influx. D-NMMA had no effect on the Ca^{2+} response to carbachol. We conclude that the NO-synthase inhibitor prevents the activation of Ca^{2+} influx by agonist, but L-NMMA does not cause Ca^{2+} release by itself and does not affect Ca^{2+} release by agonist.

Inhibition of guanylyl cyclase blocks activation of Ca^{2+} current by agonist

The guanylyl cyclase inhibitor LY83583 (Mulsch et al., 1988) blocks the activation of inward current by carbachol. In the example shown in Figure 7*A*, the cell was incubated in saline containing 10 μM LY83583 for 15 min before a saturating concentration of carbachol (1 mM) was applied in the continued presence of inhibitor. There was no effect of agonist on membrane current under these conditions. The chamber was rinsed with normal saline, and 15 min later the agonist was applied a second time. Carbachol now activated an inward current that reached 100 pA (Fig. 7*B*). In three cells tested in this way, LY83583 completely and reversibly blocked the activation of inward current by agonist (Table 1). By using Fura-2 imaging, we found that LY83583 reduces the plateau in the Ca^{2+} response, which is the expected result if Ca^{2+} influx is blocked. Figure 7*C* shows the increase in $[Ca]_i$ during stimulation with 1 mM carbachol measured after a 15 min incubation with 10 μM LY83583 (*solid line*) and again 15 min after washing the inhibitor from the chamber (*dashed line*; normalized by peak amplitude). The inhibitor had no effect on basal Ca^{2+} concentration or on the peak amplitude of the Ca^{2+} response, but it strongly reduced the plateau. This provides pharmacological evidence that the activation of inward current by muscarinic agonist requires guanylyl cyclase activity.

Rp-8-pCPT-cGMPS prevents activation of Ca^{2+} influx by agonist

The membrane-permeable cGMP analog Rp-8-pCPT-cGMPS competes with cGMP for binding sites on cGMP-dependent protein kinase and acts as a competitive inhibitor of that enzyme (Butt et al., 1994). It may act in a similar way at cGMP binding sites associated with ion channels (Kramer and Tibbs, in press), although it apparently does not affect cGMP-regulated phosphodiesterases (Butt et al., 1994). In the example shown in Figure 8*A*, the inward current in response to 1 mM carbachol was re-

corded first under control conditions and reached an amplitude of 167 pA. After 15 min in 10 μM Rp-8-pCPT-cGMPS, carbachol was applied again, and the current reached 50 pA, 30% of the control response (Fig. 8*B*). In five cells, 10 μM Rp-8-pCPT-cGMPS reduced the inward current by 73 ± 27% (mean ± SD; Table 1). Because the inhibitory cGMP analog competes with cGMP for binding sites on effector molecules, the strength of block is expected to increase with inhibitor concentration. In agreement with this prediction, we found that 15 min exposure to 100 μM Rp-8-pCPT-cGMPS prevented the activation of inward current by agonist. These data support the view that cGMP binding is necessary for activation of the current. This is supported by Fura-2 imaging experiments. Figure 8*C* shows the change in $[Ca]_i$ during the application of 1 mM carbachol under control conditions (*solid line*) and after a 15 min exposure to 100 μM Rp-8-pCPT-cGMPS. The result is representative of 10 experiments. The inhibitor had no effect on the resting Ca^{2+} concentration or on the peak change in $[Ca]_i$, which shows that it did not alter the Ca^{2+} content of internal stores or the ability of agonist to mobilize Ca^{2+}. Rp-8-pCPT-cGMPS did reduce the plateau phase of the response, which is consistent with decreased Ca^{2+} influx.

DISCUSSION

On the basis of these experiments, we conclude that cGMP is the necessary and sufficient link between muscarinic receptor activation and the activation of voltage-independent Ca^{2+} current. The same conclusion was reached for the activation Ca^{2+} influx in pancreatic acinar cells (Pandol and Schoeffield-Payne, 1990; Bahnson et al., 1993; Xu et al., 1994) and in an epithelial cell line (Bischof et al., 1995). Like the situation in acinar cells, the Ca^{2+} current in N1E-115 neuroblastoma cells is activated specifically by cGMP, and cAMP does not share this activity.

Evidence that 8-bromo-cGMP activates Ca^{2+} influx includes the following observations. The inward current is seen when cells are bathed in Na^+-free saline when Ca^{2+} is present, and in this solution the extrapolated reversal potential is consistent with a Ca^{2+} current. The cyclic nucleotide also elevates $[Ca]_i$ in Fura-2 imaging experiments, and this develops over the same time course as the inward current measured with voltage clamp. The $[Ca]_i$ increase results exclusively from Ca^{2+} influx rather than from Ca^{2+} release from internal stores. The inward current activated by 8-bromo-cGMP is blocked by external Mn^{2+} and Ba^{2+}, and this unusual ionic sensitivity is shared with the inward current activated by muscarinic agonist (Mathes and Thompson, 1994). In addition, the currents activated by 8-bromo-cGMP and by muscarinic agonist are are not additive, indicating that agonist and 8-bromo-cGMP activate the same membrane current.

Muscarinic receptor activation causes a pronounced, 16-fold increase in cGMP within 30 sec (Thompson et al., 1995). This is blocked by L-NMMA, a competitive inhibitor of NO-synthase, demonstrating that all of the guanylyl cyclase activity is attributable to the NO-sensitive form of the enzyme rather than to receptor-coupled cyclases (McKinney et al., 1990; Hu and El-Fakahany, 1993; Thompson et al., 1995). The activation of inward current by agonist is also blocked by L-NMMA without affecting IP_3 production (McKinney et al., 1990; Thompson et al., 1995). In addition, LY83583, a reversible inhibitor of guanylyl cyclase, and the cyclic nucleotide analog Rp-8-pCPT-cGMPS, a competitive inhibitor of cGMP-dependent protein kinase as well as cyclic nucleotide-gated channels (Butt et al., 1994; Kramer and Tibbs, in press), prevents the activation of inward current and Ca^{2+} influx

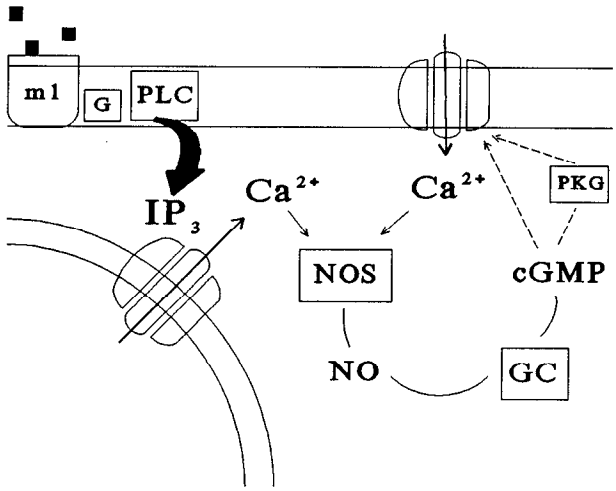

Figure 9. Model for the activation of Ca^{2+} current by muscarinic agonist. Binding of agonist to M1 receptors (*m1*) activates phospholipase-C (*PLC*) via a G-protein (*G*). The resulting increase in IP_3 concentration activates receptors associated with intracellular Ca^{2+} storage compartments to release Ca^{2+} into the cytosol. Ca^{2+} bound to calmodulin then activates NO-synthase (*NOS*), which catalyzes conversion of L-arginine to *NO* and citrulline. NO activates soluble guanylyl cyclase (*GC*) to produce *cGMP*. cGMP activates Ca^{2+} influx either by acting directly on cyclic nucleotide-gated ion channels or via an additional intermediate, for example, cGMP-dependent protein kinase (*PKG*; *dashed line*).

by agonist. None of the inhibitors affect Ca^{2+} release from internal stores or the Ca^{2+} content of stores, which shows that inhibition of cGMP production uncouples Ca^{2+}-store depletion from the activation of Ca^{2+} current.

Stimulation of NO-synthase requires Ca^{2+}/calmodulin, and cGMP production is prevented when the Ca^{2+} buffer bis(2-aminophenoxy)ethane-*N,N,N',N'*-tetra-acetic acid (or BAPTA) is introduced into the cell (Thompson et al., 1995). During the muscarinic response, NO-synthase is driven in part by Ca^{2+} released from IP_3-sensitive intracellular Ca^{2+} stores (Thompson et al., 1995), and therefore the cGMP signal has the potential to encode the depletion of Ca^{2+} stores. Maximum stimulation of cGMP production by carbachol, however, requires Ca^{2+} influx in addition to Ca^{2+} release. We found that cGMP production is reduced by 60% when Ca^{2+} influx is prevented under conditions in which Ca^{2+} release is not altered. This was interpreted as evidence that NO-synthase, or a necessary cofactor such as calmodulin, is localized to the vicinity of membrane Ca^{2+} channels (Thompson et al., 1995). Because cGMP formation is strongly dependent on Ca^{2+} influx and because Ca^{2+} influx is activated by cGMP, this pathway represents a positive-feedback loop that is critically poised to amplify the NO and cGMP signals. The feedback loop is diagrammed in Figure 9. This amplification process may explain the very rapid increase in cGMP concentration that occurs during the activation of muscarinic receptors.

The mechanism by which cGMP activates Ca^{2+} current in N1E-115 cells is not known, but there are two reasonable possibilities. cGMP might directly activate a cyclic nucleotide-gated channel, or it might act indirectly, through a cGMP-dependent kinase or phosphatase for example, to modulate Ca^{2+} channels. Cyclic nucleotide-gated channels have been described in photoreceptors, olfactory neurons, and nonsensory neurons of vertebrates (Distler et al., 1994) and invertebrates (Huang and Gillette, 1993). Members of this family of heteromultimeric proteins share sequence homology in the cGMP-binding domain, but there is

wide variability outside of this region, including variability in membrane-spanning segments thought to constitute the ion pore. This suggests that different members of the family may have different patterns of ionic selectivity or sensitivity to regulatory ligands. The inward currents activated by 8-bromo-cGMP and muscarinic agonist in N1E-115 neuroblastoma cells share several properties with cyclic nucleotide-gated channels, including the absence of voltage dependence, a conductance to Ca^{2+} that seems to saturate readily with increasing concentration (Hodgkin et al., 1985), possible Ca^{2+}-dependent inactivation or self-block (Liu et al., 1994), and lack of permeability to Ba^{2+} and Mn^{2+} when Ca^{2+} is present (Capovilla et al., 1983). A definitive test for the presence of cyclic nucleotide-gated channels in N1E-115 cells will require additional experiments.

REFERENCES

Almers W, McCleskey EW (1984) Nonselective conductance in calcium channels of frog muscle: calcium selectivity in a single-file pore. J Physiol (Lond) 353:585–608.

Amano T, Richelson E, Nirenberg M (1972) Neurotransmitter synthesis by neuroblastoma clones. Proc Natl Acad Sci USA 69:258–263.

Bahnson TD, Pandol SJ, Dionne VE (1993) Cyclic GMP modulates depletion-activated Ca^{2+} entry in pancreatic acinar cells. J Biol Chem 268:10808–10812.

Bischof G, Brenan J, Bredt DS, Machen TE (1995) Possible regulation of capacitative Ca^{2+} entry into colonic epithelial cells by NO and cGMP. Cell Calcium 17:250–262.

Butt E, Eigenthaler M, Benieser HG (1994) Rp-8-pCPT-CGMPS, a novel cGMP-dependent protein kinase inhibitor. Eur J Pharmacol 269:265–268.

Capovilla M, Caretta A, Cervetto L, Torre V (1983) Ionic movements through light-sensitive channels of toad rods. J Physiol (Lond) 343:295–310.

Distler M, Biel M, Flockrzi V, Hofmann F (1994) Expression of cyclic nucleotide-gated cation channels in non-sensory tissues and cells. Neuropharmacology 33:1275–1282.

Grynkiewicz G, Poenie M, Tsien RY (1985) A new generation of Ca^{2+} indicators with greatly improved fluorescence properties. J Biol Chem 260:3440–3450.

Hagiwara S (1983) Membrane potential-dependent ion channels in cell membrane: phylogenetic and developmental approaches. New York: Raven.

Hess P, Tsien RW (1984) Mechanism of ion permeation through calcium channels. Nature 309:453–456.

Hodgkin AL, McNaughton PA, Nunn BJ (1985) The ionic selectivity and calcium dependence of the light-sensitive pathway in toad rods. J Physiol (Lond) 358:447–468.

Horn R, Marty A (1988) Muscarinic activation of ionic currents measured by a new whole-cell recording method. J Gen Physiol 92:145–159.

Hu J, El-Fakahany E (1993) Role of intercellular and intracellular com-munication by nitric oxide in coupling of muscarinic receptors to activation of guanylate cyclase in neuronal cells. J Neurochem 61:578–585.

Huang R-C, Gillette R (1993) Co-regulation of cAMP-activated Na^{+} current by Ca^{2+} in neurones of the mollusk *Pleurobranchaea*. J Physiol (Lond) 462:307–320.

Kao JPY, Harootunian AT, Tsien RY (1989) Photochemically generated cytosolic calcium pulses and their detection by fluo-3. J Biol Chem 264:8179–8184.

Kimhi Y, Palfrey C, Spector I, Barak Y, Littauer UZ (1976) Maturation of neuroblastoma cells in the presence of dimethlysulfoxide. Proc Natl Acad Sci USA 73:462–466.

Kramer RH, Tibbs GR (1996) Antagonists of cyclic nucleotide-gated channels and molecular mapping of their site of action. J Neurosci, in press.

Liu M, Chen T-Y, Ahamed B, Li J, Yau K-W (1994) Calcium-calmodulin modulation of the olfactory cyclic nucleotide-gated cation channel. Science 266:1348–1354.

Mathes C, Thompson SH (1994) Calcium current activated by muscarinic receptors and thapsigargin in neuronal cells. J Gen Physiol 104:107–121.

Mathes C, Thompson SH (1995) The relationship between depletion of intracellular Ca^{2+} stores and activation of Ca^{2+} current in neuroblastoma cells. J Gen Physiol 106:975–994.

McKinney M, Bolden C, Smith C, Johnson A, Richelson E (1990) Selective blockade of receptor-mediated cyclic GMP formation in N1E-115 neuroblastoma cells by an inhibitor of nitric oxide synthesis. Eur J Pharmacol 178:139–140.

Mulsch A, Busse R, Liebau S, Forstermann U (1988) LY83583 interferes with the release of endothelium-derived relaxing factor and inhibits soluble guanylate cyclase. J Pharmacol Exp Ther 247:283–288.

Pandol SJ, Schoeffield-Payne MS (1990) Cyclic GMP mediates the agonist stimulated increase in plasma membrane calcium entry in the pancreatic acinar cell. J Biol Chem 265:12844–12853.

Putney Jr JW, Bird GSJ (1993) The signal for capacitative calcium entry. Cell 75:199–201.

Thompson SH, Mathes C, Alousi AA (1995) Calcium requirement for cGMP production during muscarinic activation of N1E-115 cells. Am J Physiol 269:C979–C985.

Wang SS-H, Thompson SH (1994) Measurement of changes in functional muscarinic acetylcholine receptor density in single neuroblastoma cells using calcium release kinetics. Cell Calcium 15:483–496.

Xu X, Star RA, Tortorici G, Muallem S (1994) Depletion of intracellular Ca^{2+} stores activates nitric-oxide synthase to generate cGMP and regulate Ca^{2+} influx. J Biol Chem 269:12645–12653.

Yoshii M, Tsunoo A, Narahashi T (1988) Gating and permeation of two types of calcium channels in neuroblastoma cells. Biophys J 54:885–895.